Structural characterisation of Fe_2O_3 nanoparticles

Michael Hagelstein[1], Dorothée Vinga Szabó[2], Sabine Schlabach[2], Paolo Masala[3], Marco Scavini[3], Mauro Coduri[4], Claudio Ferrero[5]
[1]Karlsruhe Institute of Technology, ANKA, Karlsruhe, Germany,
[2]Karlsruhe Institute of Technology, Institute for Applied Materials (IAM) and Karlsruhe Nano-Micro-Facility (KNMF), Karlsruhe, Germany,
[3]University of Milan, Department of Chemistry, Italy,
[4]CNR-IENI Institute for Energetics and Interphases, Lecco, Italy,
[5]ESRF-The European Synchrotron, Grenoble, France

E-mail: michael.hagelstein@kit.edu

Abstract. The structure of nano-crystalline Fe_2O_3 particles, synthesized using the microwave plasma technique, has been analysed using synchrotron based X-ray absorption spectroscopy and X-ray powder diffraction, as well as transmission electron microscopy. Furthermore, magnetic properties, the crystal structure, and the microstructures are compared and the potential model character of the samples for structure simulations is discussed.

1. Introduction

There is growing interest in the application of monodisperse magnetic nanoparticles in magnetic suspensions, ferrofluids, or for drug delivery. In general, magnetic properties of nanoparticles are observed to be size dependent, independent from the method of synthesis [1]. However, our studies with microwave plasma synthesized Fe_2O_3 nanoparticles [2] show that the magnetic properties do not always correlate with the particle sizes. Although transmission electron microscopy studies reveal quite similar particle sizes of 5 nm, the saturation magnetization differs significantly (see [3]). The reason for this discrepancy is not yet fully clear. We believe that it is intimately related to the atomic structure of the nanoparticles coupled with possible structural disorder induced by the particle size. In addition to the antiparallel coupling of the spin and the orbital moment in the maghemite structure which has been observed in Fe_2O_3/ZrO_2 core/shell particles earlier [4], competing magnetic interactions of disordered crystal sub-lattices, strain as well as surface effects may lead to frustration and

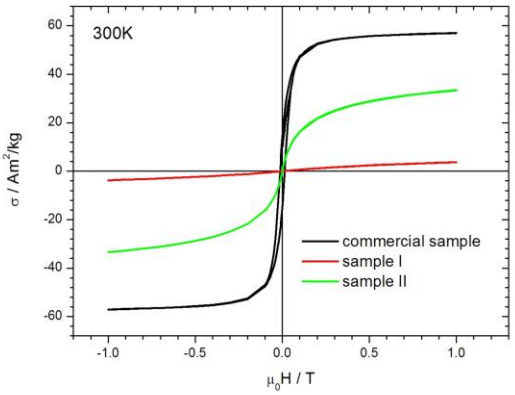

Figure 1. Magnetic moment per unit mass σ as a function of applied field $\mu_0 H$ of the samples measured at 300K.

disorder of the spin lattices. It is the aim of this paper to study the discrepancy between observed magnetization and particle size in more depth.

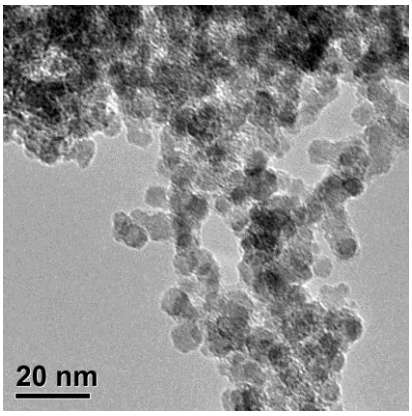

Figure 2. TEM of synthesised nanoparticles (sample II). A typical particle size of 5 nm is determined.

2. Results and discussion

We have determined the magnetic properties and performed an accurate structural and microstructural investigation of two nanocrystalline, microwave plasma synthesized Fe_2O_3 samples with similar particle size deduced by TEM and one commercial nano-Fe_2O_3 as a reference. Special emphasis is laid on X-ray absorption fine structure spectroscopy as well as high resolution X-ray powder diffraction.

2.1. Magnetic properties and transmission electron microscopy

The magnetic moment σ as a function of applied magnetic field H has been determined with a SQUID magnetometer at room temperature in the range from 1 T to -1 T. The investigated Fe_2O_3 nanoparticles are superparamagnetic and are showing different saturation magnetization. The commercial material in contrast exhibit hysteresis and a significantly higher saturation magnetization (see figure 1). A typical TEM image from microwave-plasma synthesized Fe_2O_3 is displayed in figure 2.

2.2. X-ray powder diffraction

X-ray powder diffraction measurements on samples I and II and on a γ-Fe_2O_3 reference sample were performed at room temperature at the ID31 beamline of the ESRF (now ID22). The samples were investigated at λ=0.400 Å covering a wave-vector Q region up to $Q_{max} \sim 25.7$ Å^{-1}. The experimental data have been analysed using: i) the Williamson-Hall (W-H) method [5] in order to establish the crystallite size and strain, ii) the Rietveld method to determine the average crystal structure and iii) the total pair distribution function G(r) to unveil the possible structural disorder. The last one is obtained by Fourier transforming the total scattering functions S(Q) which, in turn, is obtained by the experimental data after suitable corrections and normalizations [6].

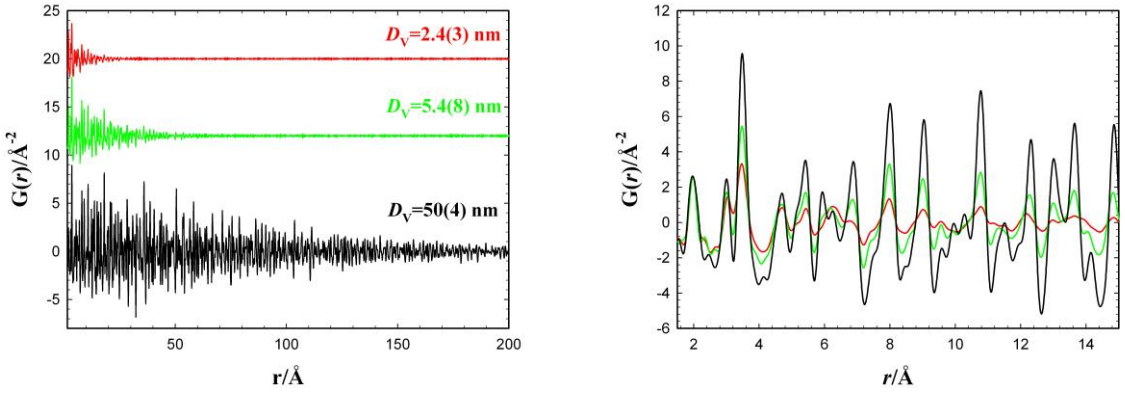

Figure 3. G(r) data collected on the γ-Fe_2O_3 samples at the ESRF. The left hand panel presents data up to 200 Å, while the right hand panel highlights the low r region. γ-Fe_2O_3 reference (black curves), sample I (red) and sample II (green).

Selected results of the Rietveld analysis are displayed in table 1. The most abundant phase in all the investigated γ-Fe_2O_3 samples is maghemite with a secondary hematite phase. The γ-Fe_2O_3 reference sample had to be refined in a tetragonal space group with a tripling of the c-axis because of ordering of

iron vacancies. Figure 3 (left) shows the G(*r*) data points on the two samples and reference sample in a large interatomic distance range.

The damping of the G(*r*) functions is related to the finite dimension of the nanoparticles and can be mapped by a spherical envelope function which supplies alternative values of the crystallite dimension (see numbers in Figure 3, left). The damping of G(*r*) is related to the average volume-weighted diameters (D_V) of the different sample crystallite sizes. On the right are depicted the same G(*r*) curves. The widths of G(*r*) peaks pertinent to the nearest-neighbors Fe-O distances at about 2 Å look quite similar for all the samples; conversely, for greater distances a broadening of the G(*r*) peaks is apparent for samples I and II, as compared to the reference sample. See e.g. the Fe-Fe distances between 3 and 4 Å. This suggests a progressive disordering of interatomic distances, by decreasing the crystallite diameter, i.e. increasing the surface/volume ratio. This finding is in agreement with the high strain parameters detected for samples I and II by the W-H analysis compared to the γ-Fe_2O_3 reference sample (see table 1).

Table 1. Crystallographic data for the γ-Fe_2O_3 reference sample and the two nano-crystalline samples obtained by the Rietveld method. Size and strain data obtained by Williamson-Hall and PDF analysis.

	γ-Fe_2O_3							α-Fe_2O_3
	Space group	**a (Å)**	**c (Å)**	**Fraction (w%)**	**D_V (W-H)**	**D_V (PDF)**	**ε**	**Fraction (w%)**
γ-Fe_2O_3 reference	$P4_12_12$	8.3463(1)	25.0269(1)	96.0(0.1)	55(5)	50(4)	0.0022(5)	4.0(0.4)
Sample I	$P4_332$	8.3464(9)	--------	80.8(6)	2.3(1)	2.4(3)	0.0095(9)	19.2(9)
Sample II	$P4_332$	8.3439(8)	--------	87.2(1)	3.8(1)	5.4(8)	0.0084(6)	12.8(7)

2.4. X-ray absorption spectroscopy

XAFS spectra have been collected at the Fe-K edge in transmission mode. Experiments were performed at the SUL-X beamline at ANKA. This beamline delivers a focused, monochromatic beam by using a wiggler source, focusing mirrors and a cryogenically cooled Si(111) double crystal monochromator. The data analysis followed a standard procedure using the code WINXAS. For the

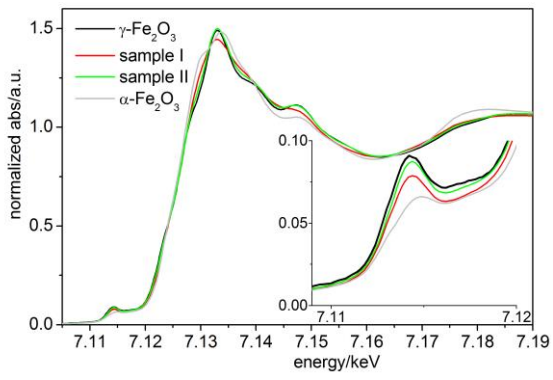

Figure 4. The near edge region of iron oxide nanoparticles (sample I, sample II) together with γ-Fe_2O_3 reference sample and α-Fe_2O_3.

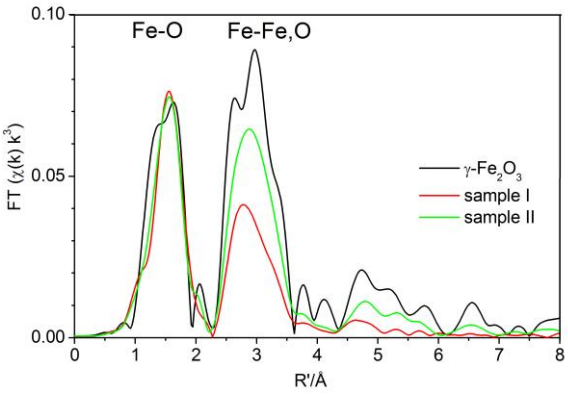

Figure 5. Fourier transforms of the XAFS (not phase shift corrected) of the sample I and II together with the γ-Fe_2O_3 reference sample.

XAFS analysis, a *k*-range of 2.4 - 14.5 $Å^{-1}$ was used for calculating the Fourier transform. The near edge structure and the Fourier transform of the XAFS are displayed in figure 4 and 5, respectively.

The XANES region with the pre edge peak assigned to a 1s to 3d transition provides valuable information on the relative occupation of tetrahedral and octahedral sites [7]. In particular, the decrease of the pre-edge peak intensity of the nanomaterials with respect to the reference sample suggests a smaller Fe_{tetra}/Fe_{oct} ratio.

XAFS analysis using $\chi(k)$ k^3 weighting with FEFF theoretical functions [8] have been calculated for the first Fe-O shell and two next nearest Fe-Fe shells using structural data from Shmakov et al. [9] and Petkov et al. [10]. Higher Fe-O coordination shells and multiple scattering paths are not included. The bond lengths R_i and coordination numbers CN_i for the coordination shells are summarized in table 2.

Table 2. Radial distances R_i (±0.01 Å) and coordination numbers CN_i (error ±10%) determined from the XAFS data (the many body amplitude reduction factor S_0^2 fixed at 0.9). The Debye-Waller factors for the next nearest Fe shells σ_2^2 and σ_3^2 have been kept fixed at 0.01 Å^2 during refinement of the three shells.

	R_1 [Å] Fe-O	**σ_1^2 [Å^2]**	**CN_1 Fe-O**	**R_2 [Å] Fe-Fe**	**CN_2 Fe-Fe**	**R_3 [Å] Fe-Fe**	**CN_3 Fe-Fe**
γ-Fe_2O_3 reference	1.92	0.012	6.2	2.99	3.1	3.42	6.9
Sample I	1.95	0.010	5.2	3.01	1.5	3.41	5.7
Sample II	1.94	0.011	5.3	3.02	3.5	3.43	6.5

3. Conclusions

This investigation reveals major structural characteristics of the synthesized samples. The samples are predominantly maghemite but with considerable fractions of hematite. Lattice parameters are comparable to the bulk; the coordination of Fe ions at the surface appears to be distorted. The site occupation ratio Fe_{tetra}/Fe_{oct} is smaller than for bulk maghemite which is also corroborated by the longer average bond length for the first Fe-O shell determined by XAFS. Although particle sizes seem similar by TEM investigations, the crystallite sizes are significantly different. At decreasing the particle size, disorder increases both allowing atomic relaxations and enhancing the ratio of tetrahedral to octahedral coordinated iron. These differences may explain the differences in magnetic properties.

Still many unanswered questions further remain, i.e. the structural differences of surface and bulk of nanoparticles are to be analysed and discussed in greater detail, whether the surface contains glassy states which would explain magnetic properties, and how particles interact with each other. We hope to reveal such issues by comparing single particle structure simulations with our experimental data.

Acknowledgments

We are particularly indebted to the ANKA and ESRF synchrotron user facilities. The scientists at ESRF, Andy Fitch and Yves Watier, as well as at ANKA, Tao Liu, Stefan Mangold, Ralph Steininger, and Stephen Doyle helped us collecting and analyzing the data.

References

[1] Szabó D V, Schlabach S 2014 *Inorganics* **2(3)** 468
[2] Vollath D, Szabó D V, Taylor R D and Willis J O J 1997 *Mater. Res.* **12** 2175
[3] Nadeem K, Krenn H, Traussnig T, Würschum R, Szabó D V, Letofsky-Pabst I 2011 *J. Magn. Magn. Mat.* **323** 1998
[4] Pellegrin E, Hagelstein M, Doyle S, Moser H O, Fuchs J, Vollath D, Schuppler S, James M A, Saxena S S, Niesen L, Rogojanu O, Sawatzky G A, Ferrero C, Borowski M, Tjernberg O, and Brookes N B 1999 *phys. stat. sol. (b)* **215** 797
[5] Williamson G K, Hall W H 1953 *Acta Metall.* **1** 22
[6] Egami T, Billinge S J L, *Underneath the Bragg peaks: Structural Analysis of Complex Materials* 2003 **V. 7** Pergamon Materials Series: Oxford
[7] Meneghini C, Boscherini F, Pasquini L, Renevier H 2009 *J. Appl. Cryst.* **42** 642
[8] Rehr J J, Kas J J, Vila F D, Prange M P, Jorissen K 2010 *Phys. Chem. Chem. Phys.* **12** 5503
[9] Shmakov A N, Kryukova G N, Tsybulya S V, Chuvilin A L, Solov'eva L P 1995 *J. Appl. Cryst.* **28** 141
[10] Petkov V, Cozzoli P D, Buonsanti R, Cingolani R, Ren Yang 2009 *J. Am. Chem. Soc.* **131(40)** 1426